Biophysical Chemistry, 45 (1992) 1–6
Elsevier Science Publishers B.V., Amsterdam

BIOCHE 01687

Tryptophan fluorescence intensity and anisotropy decays of human serum albumin resulting from one-photon and two-photon excitation

Joseph R. Lakowicz and Ignacy Gryczynski
Center for Fluorescence Spectroscopy, Department of Biological Chemistry, University of Maryland, School of Medicine,
660 W. Redwood Street, Baltimore, MD 21201 (USA)

(Received 24 March 1992, accepted in revised form 8 May 1992)

Abstract

We measured the emission spectra, intensity decays and anisotropy decays of the single tryptophan residue of human serum albumin (HSA) resulting from one-photon (295–298 nm) and two-photon (590–596) excitation. The emission spectra and intensity decays were independent of the mode of excitation. The anisotropy decays were superficially similar for one- and two-photon excitation. However, upon consideration of the different orientation photoselection for one- and two-photon excitation, the anisotropy data reveal different angles between the absorption and emission oscillators for one-photon and two-photon excitation. This result suggests different relative one-photon and two-photon cross-sections for the ^1L_a and ^1L_b transitions of the indole residue. This first report of the time-resolved anisotropy decay of a protein resulting from two-photon excitation suggests that such measurement will yield insights into the complex photophysical properties of tryptophan residues in proteins.

Keywords: Tryptophan fluorescence intensity decay; Tryptophan anisotropy decay; One- and two-photon excitation; Human serum albumin

1. Introduction

Time-resolved measurements of the intensity and anisotropy decays of the intrinsic tryptophan fluorescence of proteins are widely utilized to study the structure and dynamics of proteins [1,2]. To date, such measurements have relied almost exclusively on one-photon excitation (OPE) of fluorescence. However, excitation of fluorescence by simultaneous absorption of two-photons, here called two-photon excitation (TPE), is known to follow different selection rules and thus probe electronic states and/or transitions normally invisible to one-photon spectroscopy [3–6]. Two-photon spectroscopy has been used to investigate a variety of chromophores [6–8], and the differential absorption of linear and circular polarized light has been used to investigate the electronic properties of indoles [9,10]. To date, there is only

---

Correspondence to: Dr. J.R. Lakowicz, Center for Fluorescence Spectroscopy, Department of Biological Chemistry, University of Maryland, School of Medicine, 660 W. Redwood Street, Baltimore, MD 21201, USA.

a single report of the steady state emission spectra of proteins observed for two-photon excitation [11], and there have been no reports of the time-resolved emission of proteins resulting from two-photon excitation. In the present report, we described frequency-domain measurement of the intensity and anisotropy decays resulting from OPE and TPE of the single tryptophan residue in human serum albumin (HSA).

2. Experimental methods

HSA obtained from Calbiochem (> 99%), lot number 126658, was used without further purification. To facilitate comparison of the OPE and TPE experimental data, we used the same concentration of HSA (67 mg/ml or 10^{-3} M) for the OPE and TPE experiments, in 50 mM tris 100 mM NaCl, pH 8, 20°C. The HSA fluorescence emission was observed through Schott WG320 and Corning 7-54 filters, which blocked scattered light for both one- and two-photon excitation.

Single photon excitation was accomplished using the frequency-doubled output of a cavity-dumped rhodamine-6G laser at 295 to 298 nm. For two-photon excitation we used the fundamental output from 590 to 596 nm, which was focused in the sample using a 5 cm focal length lens. For both OPE and TPE, the pulse width was about 5 ps at a repetition rate of 3.795 MHz. Signal from the solvent alone was less than 0.5% for both one- and two-photon excitation. Steady state anisotropy spectra were obtained in the usual L-format manner [12].

Because of the high concentration and absorbance of HSA, it was not possible to use the usual right-angle geometry with the focal point in the center of the cuvette. For OPE we used 0.5 cm × 0.5 cm cuvettes with excitation and emission located near a corner of the cuvette. This cuvette was positioned off center in a 1 cm × 1 cm cuvette holder. For the TPE, we used 1.0 × 0.5 cm cuvettes, with the long axis aligned along the incident light path and with the focal point positioned about 0.5 cm from the surface facing the incident light. The position of the cuvette and the lens were adjusted so that the focal point of the laser excitation was located near the observation window.

Frequency-domain intensity and anisotropy decays were obtained on the GHz instrument described previously [13,14]. Intensity decays were measured using magic-angle conditions. Intensity decays ($I(t)$) were fit to the multi-exponential model using

$$I(t) = \sum_i \alpha_i \, e^{-t/\tau_i} \tag{1}$$

where α_i are the amplitudes associated with the decay time τ_i. The mean decay time $\langle\tau\rangle$ is given by $\langle\tau\rangle = \Sigma_i \alpha_i \tau_i^2$. The differential phase and modulated anisotropy data were fit to the multi-correlation time anisotropy decay ($r(t)$) model using

$$r(t) = \sum_j r_{0j} \, e^{-t/\theta_j} \tag{2}$$

where r_{0j} is the amplitude of the total anisotropy ($r_0 = \Sigma r_{0j}$) which decays with a correlation time θ_j.

The frequency-domain intensity and anisotropy decays were analyzed as described previously [15–17]. For analysis of the intensity decays the uncertainties in phase and modulation were assumed to be 0.2° and 0.005, respectively. For analysis of the anisotropy decays the same uncertainties were assumed for the differential polarized phase (Δ) and modulation ratios (Λ), respectively [17].

3. Theory

In previous reports, we described the steady state and time-resolved anisotropy decays of molecules with collinear absorption and emission dipoles from OPE and TPE [18,19]. For such molecules, the value of r_0 is near 0.40 for OPE. However, the value of r_0 for TPE was found to be larger on 0.40, apparently because TPE depends on $\cos^4\theta$, where θ is the angle between the electronic vector of the incident light and the absorption transition moment of the fluorophore. In contrast, the absorption probability for OPE depends on $\cos^2\theta$. This difference can be regarded as a trivial, i.e, non-molecular effect, of comparing OPE and TPE anisotropy data. Suppose a fluorophore is motionless between excitation and emission, and that the angle β describes the angle between the absorption and emission moments. The anisotropy is then given by

$$r^1(\beta) = \tfrac{2}{5}\left(\tfrac{3}{2}\cos^2\beta - \tfrac{1}{2}\right) \tag{3}$$

and

$$r^2(\beta) = \tfrac{4}{7}\left(\tfrac{3}{2}\cos^2\beta - \tfrac{1}{2}\right) \tag{4}$$

where the superscripts ^{1} and ^{2} refers to OPE and TPE, respectively. Hence, the individual data sets for OPE or TPE can be analyzed using eqs. (3) or (4), respectively, to recover the angle β. If the values of β are different, then the data suggests different relative absorbance of the ^1L_a and ^1L_b transitions. Alternatively, the OPE and TPE data sets can be analyzed globally to determine whether they are consistent with a single value of β.

4. Results and discussion

4.1 Emission spectra of HSA

Emission spectra of HSA are shown in Fig. 1. Essentially the same emission spectra were observed for one- (– – –) and two-photon (———) excitation. At this time, we do not know if the small change in spectral shape is significant. The HSA emission showed a quadratic dependence (Fig. 2) on the incident intensity at 590 nm (●), but linearly dependent in intensity at 295 (○). This quadratic dependence on intensity demonstrates that the observed emission was in fact due to a biphotonic process at 590 nm.

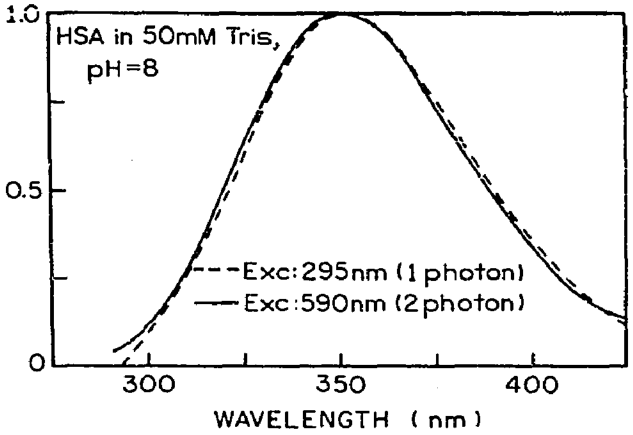

Fig. 1. Fluorescence emission spectra of human serum albumin for excitation at 295 (– – –) and 590 nm (———).

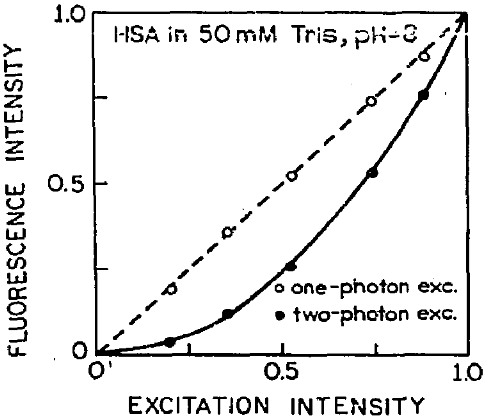

Fig. 2. Dependence of the fluorescence intensity of HSA on the excitation intensity at 295 (○) and 590 nm (●).

4.2 Intensity decays of HSA

The frequency-response of the HSA emission is shown in Fig. 3 for OPE (top) and TPE (bottom). The frequency responses for OPE and TPE were essentially identical, or can be seen from the mean decay time ($\langle\tau\rangle$) and the α_i and τ_i values from the double-exponential fit (Table 1). We do not feel the small decrease in $\langle\tau\rangle$ is significant, but similar small decreases in the mean decay times of 1,6-diphenylhexatriene [15] and 2,5-diphenyloxazole [16] were observed for TPE. We note that the values of χ^2_R for a frequency-domain analysis depend on the assumed uncertainties and are not necessarily near unity [15–17]. The values of χ^2_R did not decrease further for a triple-exponential fit, which indicates that two decay times are adequate to account for the present data.

4.3 Anisotropy decay of HSA

In contrast to the frequency-domain (FD) intensity decays, the FD anisotropy data for HSA

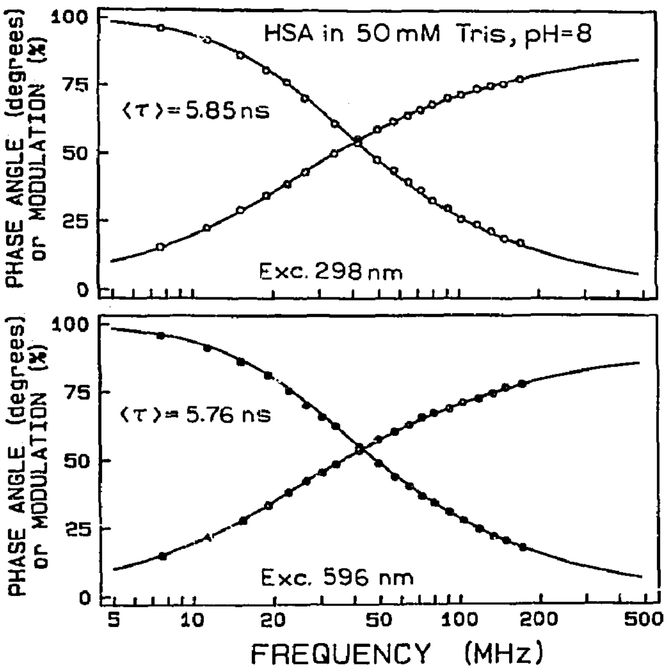

Fig. 3. Frequency-response of the intrinsic tryptophan emission of HSA for one-photon (top, ○) and two-photon (●) excitation. The solid lines represent the best two-exponential fit to the data (Table 1).

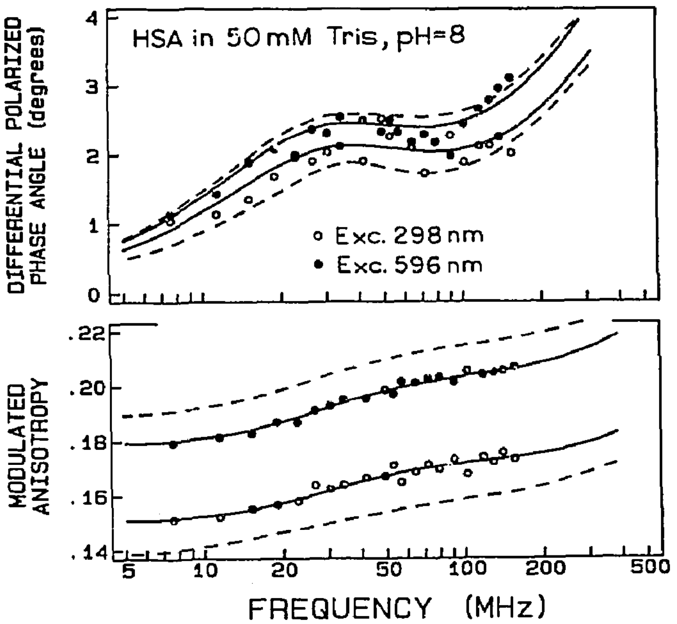

Fig. 4. Frequency-domain anisotropy data for the tryptophan emission from HSA for excitation at 298 (○) and 596 nm (●). The solid lines represent the best two-correlation time fits to the data assuming independent values of r_0 at each excitation wavelength. The dashed lines represent the best fit assuming the r_0 value for 298 and 596 nm are linked by eqs. (3) and (4).

are markedly different for OPE and TPE (Fig. 4). The differential phase angles are comparable in magnitude (top) but the modulated anisotropies are distinct (bottom). When analyzed individually, the OPE and TPE data yield nearly identical correlation times (Table 2). The values of χ^2_R did not decrease further for a three correlation time fit, so that the slightly elevated value of χ^2_R for the OPE anisotropy analysis is the result of somewhat larger random error in this particular data set.

As is typical for tryptophan residues in proteins, the anisotropy decay contains a short correlation time due to segmental motions of the tryptophan residue, and a longer correlation time reflecting overall rotational diffusion of the protein. However, the initial anisotropies, whether obtained from the FD data ($r_0 = \Sigma r_{0i}$) or from

Table 1

Multi-exponential analysis of the HSA intensity decays resulting from one- or two-photon excitation

Excitation	$\langle\tau\rangle$ [a] (ns)	τ_i (ns)	α_i (ns)	f_i [b]	χ^2_R
One-photon		1.42	0.159	0.043	–
298 nm	5.85	6.06	0.841	0.957	1.7
Two-photon	5.76	2.12	0.270	0.112	–
596 nm		6.22	0.730	0.888	1.9

[a] $\langle\tau\rangle = \Sigma_i f_i \tau_i$.

[b] $f_i = \alpha_i \tau_i / \Sigma_j \alpha_j \tau_j$.

Table 2

Anisotropy decay analysis of HSA fluorescence in 50 m*M* Tris, pH 8 at 20°C

Excitation	β (deg)	r_{0i}	θ_i (ns)	χ^2_R
One-photon	30	0.074	0.17	–
298 nm		0.170	38.6	2.2
Two-photon	36	0.075	0.21	–
596 nm		0.201	38.4	1.0
Global one-	34.6	0.058	0.19	–
and two-photon		0.149	38.6	111.2

Table 3

Comparison of the initial anisotropies (r_0) and HSA[a] and indole derivatives [b] for one-photon and two-photon excitation [c]

Compound	OPE at 298 nm	TPE at 596 nm [d]	Expected [e]
Indole	0.29	0.31	0.41
NATA	0.30	0.17	0.43
Trp	0.30	0.18	0.43
2,3-Dimethyl indole	0.32	0.28	0.46
5-Methoxy indole	0.28	0.10	0.40
HSA	0.25	0.28	0.36

[a] 70% (v/v) Propylene glycol/water, −60°C.

[b] Propylene glycol, −60°C.

[c] The OPE and TPE measurements of each compound were performed on the same solution, using the geometry described in Section 2. The fluorophore concentrations were in the range of 5×10^{-4} to 2×10^{-3} *M*.

[d] Observed value.

[e] Expected value assuming $r_0^2 = \frac{10}{7} r_0^1$.

measurement in vitrified solutions (Table 3), are not related by the expected factor of 10/7 obtained by comparison of eqs. (3) and (4). This suggests that the values of β are different for OPE and TPE. We note that the anisotropy data for OPE and TPE were obtained using the same HSA sample and same HSA concentration. Also, the size of the HSA molecule precludes close contact between the tryptophan residues. For this reason energy transfer between the single tryptophan residue in each HSA molecule is unlikely. Further evidence against any effects of energy transfer or cuvette geometry is that other results with colinear oscillators [18–19] resulted in the expected increase in anisotropy resulting from $\cos^4\theta$ versus $\cos^2\theta$ photoselection.

To evaluate the apparent values of β, the FD anisotropy data were analyzed in terms of eqs. (3) and (4), for the OPE and TPE data, respectively. Since the values of r_0 can be altered by changes in the value of β, the goodness-of-fit (χ_R^2) values are the same as found using eq. (2). However, the values of β are different for OPE and TPE. Additional support for different effective β values for OPE and TPE is seen from our attempt to analyze both types of data with the single value of β. This attempt resulted in an extremely poor fit (see Fig. 4, – – –) and a 50- to 100-fold increase in the value of $\chi_R^2 = 111.2$ (Table 2). Hence, the electronic transitions contributing to the values of r_0 are differentially weighted in the OPE and TPE experiments.

4.4 Steady state anisotropies of HSA and indole derivatives

We questioned whether the OPE and TPE values of other indole derivatives were linked by the photoselection factor of 10/7. Hence, we examined the OPE and TPE steady state anisotropies (r_0^1 and r_0^2) of indole derivatives and HSA in frozen solution (Table 3). In all cases, the value of r_0^2 was not 10/7 larger than r_0^1. In some cases, r_0^2 was less than r_0^1. These data strongly suggest that either the relative absorbance of the ^1L_a and ^1L_b transitions are different for OPE and TPE, or that additional states are probed by the TPE experiment. We note that these OPE and TPE anisotropies were measured on the same solution at the same fluorophore concentration. At this concentration of 2 m*M* or lower, in polar solution, where there exists a significant Stokes' shift, energy transfer between the indole derivatives will not be significant. Also, OPE anisotropy measurements in more dilute solution yield identical anisotropy values. For all these reasons we believe energy transfer between the indole derivatives and/or geometric effects are not significant for the OPE and TPE measurements.

5. Discussion

At first examination, one may feel troubled by an inability to explain the OPE and TPE data using the expected scale factor which accounts for one-photon and two-photon photoselection. However, we now recognize that these results indicate that the OPE and TPE data either probe different electronic transitions of proteins, or different cross sections for the transitions. In either event, this indicates that the TPE data contains different information from the OPE data. Consequently, time-resolved two-photon spectroscopy of proteins contains new information on the photophysics of protein and can provide a crucial test of models describing the electronic spectra of tryptophan residues in proteins.

Acknowledgements

The authors acknowledge support from the National Science Foundation (DIR-8710401 and DMB-8804931), the National Institutes of Health (RR-04800 and RR-07510) and the Medical Biotechnology Center and Graduate School at the University of Maryland. We thank Dr. Badri Maliwal for his assistance with the preparation of the samples.

References

1 D.M. Jameson and G.D. Reinhart, eds., Fluorescent biomolecules: Methodologies and applications, (Plenum Press, New York, NY, 1989), 461 pp.
2 J.R. Lakowicz, ed., Proc. SPIE, Time-resolved laser spectroscopy in biochemistry III, Vol. 1640, (SPIE, Bellingham, WA, 1992) 807 pp.
3 W.M. McClain, Acc. Chem. Res. 7(5) (1974) 129–135.
4 R.R. Birge, in: Ultrasensitive laser spectroscopy, ed. D.S. Kliger (1983) pp. 109–174.
5 W.M. McClain, J. Chem. Phys. 55(6) (1971) 2789–2796.
6 M.J. Wirth, A.C. Koskelo, C.E. Mohler and B.L. Lentz, Anal. Chem. 53 (1981) 2045–2048.
7 M.B. Masthay, L.A. Findsen, B.M. Pierce, D.F. Bocian, J.S. Lindsey and R.R. Birge, J. Chem. Phys. 84(7) (1986) 3901–3915.
8 B. Hudson, Annu. Rev. Phys. Chem. 25 (1974) 437–460.
9 B.E. Anderson, R.D. Jones, A.A. Rehms, P. Ilich and P.R. Callis, Chem. Phys. Lett. 125(2) (1986) 106–112.
10 A. Rehms and P.R. Callis, Chem. Phys. Lett. 140(1) (1987) 83–89.
11 S.-P. Jiang, S.-H. Lian, K.-C. Ruan, L.-K. Hui, S.-H. Liu, Z. Zhang and Q. Li, Chem. Phys. Lett. 104(1) (1984) 109–111.
12 J.R. Lakowicz, Principles of fluorescence spectroscopy (Plenum Press, New York, NY, 1983) pp. 126–128.
13 J.R. Lakowicz, G. Laczko and I. Gryczynski, Rev. Sci. Instrum. 57 (1986) 2499–2506.
14 G. Laczko, I. Gryczynski, Z. Gryczynski, W. Wiczk, H. Malak and J.R. Lakowicz, Rev. Sci. Instrum. 61 (1990) 2331–2337.
15 J.R. Lakowicz, G. Laczko, H. Cherek, E. Gratton and M. Limkeman, Biophys. J. 46 (1984) 463–477.
16 E. Gratton, M. Limkeman, J.R. Lakowicz, B.P. Maliwal, H. Cherek and G. Laczko, Biophys. J. 46 (1984) 479–486.
17 B.P. Maliwal and J.R. Lakowicz, Biochim. Biophys. Acta 783 (1986) 161–172.
18 J.R. Lakowicz, I. Gryczynski and E. Danielsen, Chem. Phys. Lett. 191 (1992) 46–53.
19 J.R. Lakowicz, I. Gryczynski, Z. Gryczynski, E. Danielsen and M.J. Wirth, J. Phys. Chem. 96 (1992) 3000–3006.